

# PROBLEMS RELATED TO THERMAL FATIGUE OF STAINLESS STEEL: INTERACTIONS OF ORTHOGONAL CRACKS NETWORKS UNDER BIAXIAL TENSION AND INFLUENCE OF STRESS BIAXIALITY ON 3D MODE I CRACK GROWTH.

A.Kane, V.Doquet

Laboratoire de Mécanique des Solides, UMR-CNRS 7649

Ecole Polytechnique, 91128 Palaiseau cedex, France

doquet@lms.polytechnique.fr

## Abstract

The influence of load biaxiality on Mode I propagation of semi-elliptical fatigue cracks in 304L stainless is investigated experimentally and numerically, through 3D finite element simulations with node release. Biaxial tension is shown to reduce crack closure and accelerate crack growth in 3D, while the reverse occurs when a compressive stress is applied in the crack plane. A numerical study of the interactions between multiple cracks under biaxial tension shows that predictions ignoring the presence of orthogonal cracks would be non-conservative. The high mode-mixity ratios induced by crack interactions in a network is beneficial, since the crack roughness due to repeated bifurcations should increase asperity-induced closure and thus reduce the crack growth rates.

## Introduction

Turbulent mixing of hot (up to 170°C) and cold (25°C) water in 304L stainless steel pipes of nuclear power plants was observed to generate orthogonal networks of thermal fatigue cracks on the inner surface of some pipes. The risk of through-crack development from such superficial cracks networks has to be evaluated. Two aspects of this complex problem are considered in this study.

First, thermal loading is biaxial and the cracks growing perpendicular to the first principal stress also undergo a cyclic stress in their plane. While several studies in the literature were devoted to non singular stress effects on 2D fatigue crack growth (see for example [1-2]), to the authors best knowledge, only three papers [4-6] deal with the growth of semi-elliptical cracks under biaxial loading. A study by Shanyavskii [4] on an aluminium alloy concludes that the growth rates of semi-elliptical and through-cracks show opposite dependences with the biaxiality ratio  $\lambda = \sigma_2/\sigma_1$ . It increases when  $\lambda$  decreases for a through-crack but increases with  $\lambda$  for a surface crack. Results by Joshi et al [5] also suggest that the higher  $\lambda$ , the faster the propagation of surface cracks. An experimental and numerical investigation of this problem was thus undertaken and the results are presented in the first part of this paper.

The second aspect of the problem investigated is related to multiple fatigue cracking. Most existing approaches of the present problem [7,8] consider a through-thickness section of the pipes with edge cracks on the inner surface and either assume plane strain/stress (and straight through-cracks) or axisymmetrical configuration (with circular crack fronts). The main advantage of these models is their ability to take into account the steep gradient in stresses

due to thermal fluctuations on the inner surface and the resulting deceleration and arrest of cracks. On the other hand, they allow only uniaxial loading and stacked parallel cracks to be considered, so that only shielding effects are predicted. However, in the present thermal fatigue problem, two sets of mutually perpendicular cracks are often formed and the influence of the second set of cracks has to be assessed. A numerical approach of this question is presented in the second part of the paper.

## **Growth of semi-elliptical cracks under biaxial fatigue.**

### *Experimental study*

The material investigated is 304L austenitic stainless steel ( $\sigma_{0.2\%} = 192\text{MPa}$ ). Ten millimeter-thick disks, 100mm in diameter, containing a central semi-elliptical notch ( $c = 6\text{mm}$ ,  $a = 4\text{mm}$ , notch root radius about  $160\mu\text{m}$ ) are used. Two types of fatigue crack growth tests have been developed to investigate the influence of stress biaxiality (Fig.1).

First, diametric compression tests (Fig.1a) provide data on mode I crack growth in presence of a cyclic compression in the crack plane. The tests are performed at 5 or 10Hz, with constant maximum load and zero  $K_{\min}$ . Surface growth rates are obtained through direct measurements with a traveling microscope, while the growth rates in depth are deduced from SEM observations of crack front marks generated by R ratio variations during the tests.

Stress intensity factors at the surface and deepest points of the semi-elliptical crack were obtained through 3D finite elements computations (virtual crack advance method) considering one quarter of disk (owing to existing symmetries) loaded by a Hertzian pressure distribution on a flat part along the external border.

Closure effects are evaluated at the deepest point and surface point using a back-face strain gage and a clip-on extensometer straddling the crack, respectively. Direct observation of crack faces displacements on smaller specimens (50mm in diameter, 5mm thickness) equipped with microgrids ( $4\mu\text{m}$  pitch) compressed in a scanning electron microscope also provided an estimate of  $K_{\text{opening}}$  (Fig.2) at the free surface. Beyond the first millimeter of crack growth, in situ observations and COD measurements both yield  $K_{\text{closure}}/K_{\text{max}} = 0.3 \pm 0.03$  at the surface, while back face measurements indicate that  $K_{\text{closure}}/K_{\text{max}} = 0.09 \pm 0.03$  in depth.

An initial deceleration during the first millimetre of crack growth, followed by normal evolution of  $da/dN$  with  $\Delta K_I$  is observed, at the surface as well as in depth (Fig.3a). It was checked that this deceleration is not due to a notch effect. The stress distribution along the vertical symmetry plane computed in the uncracked specimen was used for F.E. computations of stress intensity factors in depth and surface, with a mesh representing a rectangular plate (same thickness and width as disk specimens) with a semi-elliptical notch and semi-elliptical crack loaded in tension. No decrease in  $\Delta K_I$ , which could have explained the observed deceleration is obtained for the corresponding crack dimensions. The deceleration is thus a "small-crack-like" effect, due to an increase in closure load, because of the progressive development of the plastic wake. Song and Shieh [9] recently reported a similar effect (decrease in the effective part of  $\Delta K_I$  due to wake development) during the first three millimetres of propagation of surface cracks in AISI 4130 steel. When a closure correction is applied, the growth rates measured at the free surface for semi-elliptical cracks seem to be higher than those of through-cracks submitted to uniaxial loading in CT specimens, for the

same effective  $\Delta K$  (Fig.3b). Additional measurements are needed to conclude whether or not this is an effect of load biaxiality.

Biaxial flexion of the same disks (supported by a circular ring and loaded by a smaller concentric circular ring, Fig.1b) will provide data on mode I crack growth with a cyclic tension in the crack plane. Crack growth tests due to repeated thermal shocks on the same disks are also being developed in order to determine whether crack growth kinetics measured in biaxial isothermal mechanical loading can be used to predict the 3D crack development in thermal fatigue.

### *Numerical study*

A numerical evaluation of closure effects along the front of a semi-elliptical crack under biaxial loading is attempted through elastic-plastic finite element simulations with periodic node release to take account of the plastic wake. A similar procedure has been developed by various authors [10-13] but only for uniaxial loading. Elastic-plastic constitutive equations with isotropic and non-linear kinematic hardening were fitted to experimental stress-strain curves.

The flow criterion and flow rule- where  $J_2$  denotes the second invariant of the stress deviator,  $\underline{\underline{X}}$  a nonlinear kinematic hardening variable and  $R$  an isotropic hardening variable- are:

$$\mathbf{f} = J_2(\underline{\underline{\sigma}} - \underline{\underline{X}}) - R = 0, \quad d\mathbf{f} = 0 \quad (1)$$

$$\underline{\underline{\dot{X}}} = C \underline{\underline{\dot{\epsilon}}}_p - \gamma \underline{\underline{X}} \dot{p} \quad \text{where } \dot{p} = \sqrt{\frac{2}{3} \underline{\underline{\dot{\epsilon}}}_{vp} : \underline{\underline{\dot{\epsilon}}}_{vp}} \quad (2)$$

$$R = k_0 + Q(1 - \exp(-bp)) \quad (3)$$

$$\underline{\underline{\dot{\epsilon}}}_p = \lambda \frac{\partial \mathbf{f}}{\partial \underline{\underline{\sigma}}} \quad (4)$$

where  $\lambda$  is determined from (1). The material constants in (1-4) are gathered in Table 1.

TABLE 1. Material constants used in constitutive equations

E (MPa)	k0 (MPa)	b	Q (MPa)	C (MPa)	$\gamma$
196000	165	4	180	24000	335

A semi-elliptical crack in a plate of finite thickness,  $t$ , but "infinite" height and width submitted either to an opening stress  $\sigma$  alone or opening stress plus tension or compression  $\pm \sigma$  parallel to the free surface is considered. The crack front is assumed self-similar, that is: the initial crack aspect ratio  $a/c = 0.5$  is kept constant during node release. Past the first cycle, one element is released at each subsequent cycle, at  $K_{max}$  (Fig.4). During crack "propagation", the  $a/t$  ratio varies from 0.1 to 0.105. Figure 4 shows the mesh used for all biaxiality ratios. There are at least ten linear elements (with equal height and width) in the initial plastic zone ahead of the crack front. The applied stress level,  $\sigma$ , is 65% of the micro-yield stress  $k_0$  so that small-scale yielding conditions prevail, even when the stress parallel to the crack is compressive.  $K_{closure}$  corresponds to the load for which the opening displacement of the first node behind the crack front becomes less than  $10^{-7}$  at unloading. Unilateral contact conditions are enforced to avoid crack surface interference.

Figure 5 compares the computed evolution of  $K_{closure}/K_{max}$  at the free surface and in depth, for the three loading cases considered, as the crack propagates. In accordance with previous

numerical studies [10-13], closure is more pronounced at the free surface than in depth, because crack tip plasticity is more widespread in plane stress than in plane strain and leads to slower propagation there, consistently with our experimental observations.

Furthermore, closure is predicted to be highest in shear and smallest in equibiaxial tension, which is consistent with experimental results by Shaniavskii [4] and Joshi et al. [5] (fastest crack propagation in biaxial tension, slowest in shear).

However, as shown by Table 2, the ratio of effective  $\Delta K$  at the free surface and in depth is almost unchanged, whatever the biaxiality, so that the crack aspect ratio should not depend on the type of loading. This is perfectly consistent with experimental observations by Shaniavskii [4] and Kitaoka et al [6].

TABLE 2. Computed closure

	shear	uniaxial tension	equibiaxial tension
$\Delta K^{\text{effectif}}/\Delta K^{\text{nominal}}$ free surface	0.624	0.696	0.727
$\Delta K^{\text{effectif}}/\Delta K^{\text{nominal}}$ in depth	0.886	0.975	1.00
$\Delta K^{\text{effectif}}$ depth/ $\Delta K^{\text{effectif}}$ surface	0.704	0.713	0.727

### Interaction of orthogonal crack networks under biaxial tension.

2D F.E. computations of stress intensity factors were performed for two perpendicular cracks of equal length  $L$  with one of the tips located at a distance  $d$  from the plane of the other crack, in an elastic plate under equibiaxial tension.  $K_I$  values computed on the closest tips and normalised by  $K_I$  for the isolated crack are plotted versus  $d/L$  on Fig.6. A large amplification effect (30 to 60% increase in  $K_I$  compared to an isolated crack) is found.

An orthogonal network of 19 cracks, was also considered (Fig 7) and S.I.Fs were computed on each of the 38 tips, either taking into account the whole network, or considering only the parallel cracks sub-network (in order to estimate the error due to the latter procedure). Fig 8a shows the amplification or shielding effect of parallel and orthogonal networks on  $K_I$ . A majority of crack tips are shielded (the average normalised  $K_I$  are 0.75/0.787 for parallel/ respectively orthogonal network) but amplification occurs for 25 to 30% of the crack tips (either crack tips on the border of the cracked zone, due to less shielding plus a kind of "load transfer" effect, or parallel coplanar cracks, or cracks with an orthogonal neighbour). Such amplifications would not be described if a through-thickness section had been considered.

The average ratio of  $K_I$  in the biaxial crack network to  $K_I$  in the parallel sub-network for each individual crack tip is 1.39. Ignoring the second set of cracks would thus lead to underestimate  $K_I$  and thus to non-conservative predictions of the remaining life (not to mention the fact that orthogonal cracks are likely to induce coalescence between parallel cracks that would otherwise be too faraway to interact and link). Figure 8b shows the mode-mixity ratio,  $K_{II}/K_I$ , computed for each of the 38 crack tips, either in the orthogonal network or in the parallel sub-network. This ratio exceeds 20% for many cracks, which implies (assuming that the local symmetry criterion [14] is followed) their bifurcation by more than  $29^\circ$ . The beneficial influence of multiple cracking, generally attributed merely to shielding effects has an additional origin: crack path roughness due to repeated bifurcations should reduce the crack growth rates because of asperity-induced closure.

In order integrate this effect, numerical simulations of the development of interacting cracks in an orthogonal 2D network submitted to biaxial tension based on: 1) F.E. computations of mode I and mode II S.I.Fs, 2) application of the local symmetry criterion to

determine bifurcation angles, 3) stepwise integration of Paris law and 4) treatment of coalescences between initially parallel or perpendicular cracks are being developed. Figure 9 shows an application of these simulations to the coalescence of parallel offset cracks submitted to remote tension. A stochastic procedure to describe the continuous initiation of new cracks will also be added.

Similar simulations of semi-elliptical cracks network development based on 3D F.E. computations can be envisaged and would allow consideration of thermal stress gradients in depth as well as of orthogonal networks. However, unless advanced techniques like X.F.E.M. be used, it would be impossible to take bifurcations and crack roughness into account. Anyway, since crack roughness has a beneficial impact on the fatigue life, such simulations, considering only mode I growth of plane 3D cracks should be conservative.

## Conclusions.

-Contrary to the tendency for 2D through-cracks, biaxial tension reduces crack closure for surface cracks, while the reverse occurs for a parallel compressive stress.

-The detrimental influence of orthogonal cracks should not be ignored in biaxial tension.

-The beneficial influence of multiple cracking is partly due to interactions-induced mode mixity, which increases asperity-induced closure.

Acknowledgments: Financial support for his study is provided by EDF.

## References

1. Miller, K.J., Brown, M.W., In *Multiaxial fatigue*, ASTM STP 853, edited by K.J.Miller and M.W.Brown, ASTM, Philadelphia, 1985, 135-152
2. Hoshida, T., Tanaka, K., Yamada, Y., *Fat.Fract.Eng.Mat.Struct.*, vol. **4**,355-366, 1981
3. Mc Clung, R.C., *Fat. Fract. Eng. Mat. Struct.*, Vol. **5**, 447-460, 1989
4. Shanyavskii, A.A., *Fat.Fract.Eng.Mat. Struct.*, Vol **19** N°**12**, 1445-1458, 1996
5. Joshi, S.R., Shewchuk, J., *Experimental Mechanics*, 529-533, dec.1970
6. Kitaoka, S., Mikuriya, T., *Int.Journ.Fatigue*, vol.**18** N°**3**, 205-211, 1996
7. Maillot, V., Fissolo, A., Degallaix, G. and S, Marini, B., Le Roux, J.C., In *Proceedings ECF14*, Cracovie, 2002, 425-434
8. Seyedi, M., Hild, F., Taheri, S., In *proceedings Fatigue 2002*, Stockholm, edited by A.F.Blom, EMAS, vol.3, 1735-1742
9. Song P.S, Shieh Y.L., *Int.Journ.Fatigue*, vol. **26**, 429-436, 2004
10. Chermahini, R.G., Palmberg, B., Blom, A.F., *Int.Journ. Fatigue*, vol.**15**, 259-263, 1993
11. Roychowdhury, S. Dodds, R.H. Jr, *Eng.Fract.Mech*, Vol. **70**, 2363-2383, 2003
12. Zhang, J.Z., Bowen, P., *Eng.Fract.Mech.*, vol. **60**, pp341-360, 1998
13. Skinner, J.D., Daniewicz, S.R., *Eng.Fract.Mech.*, vol. **69**, pp1-11, 2002
14. Amestoy, M, Bui, H.D, Dang Van, K, *C.R. Acad. Sci. Paris*, vol. **B289**, 99-102, 1979

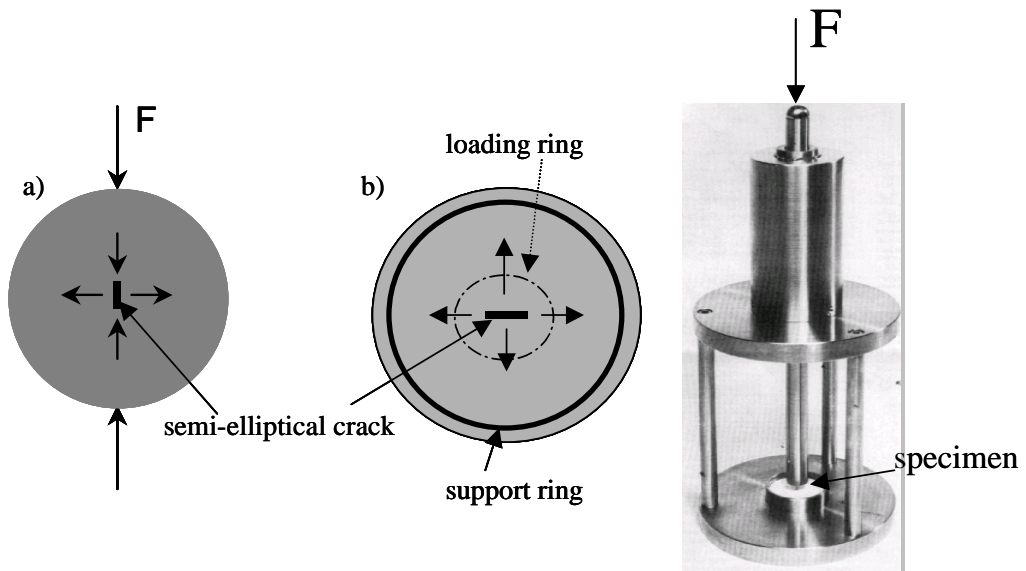


FIGURE 1. Tests under biaxial loading. a) diametric compression b) biaxial bending

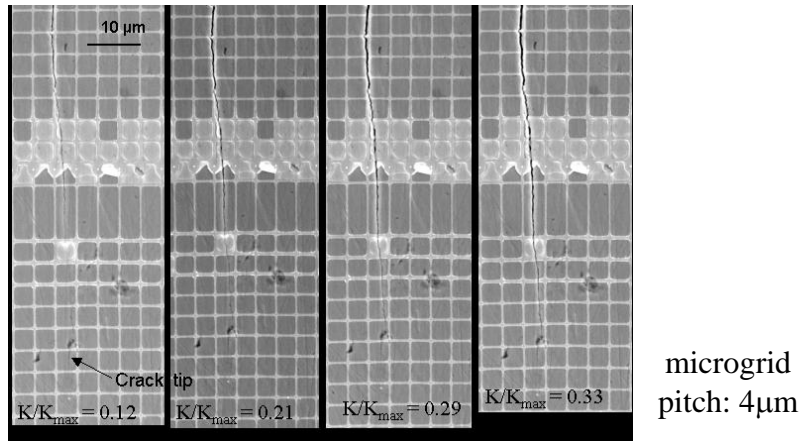


FIGURE 2. Estimation of  $K_{opening}$  at the free surface by loading a specimen in the SEM

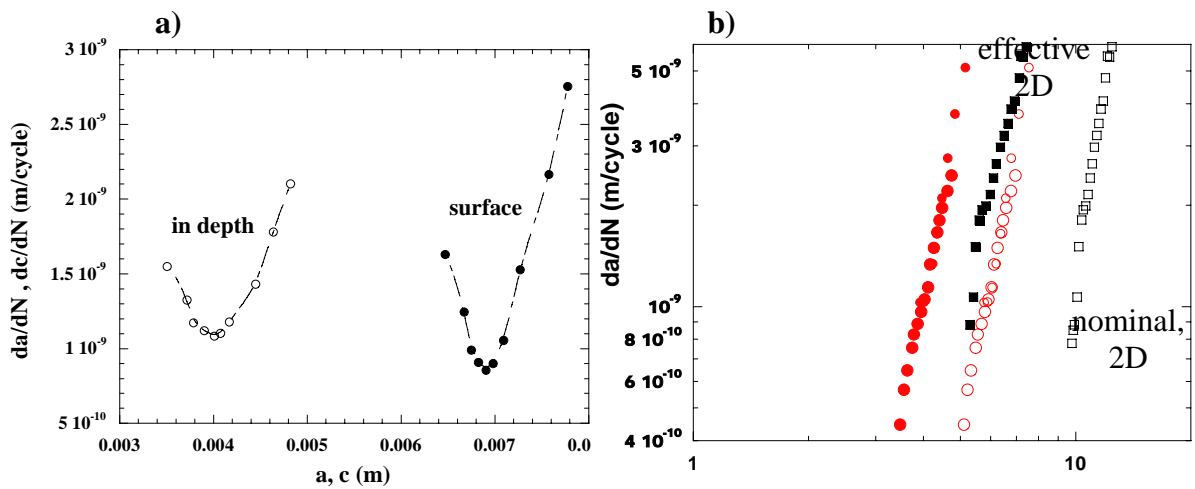


FIGURE 3. Crack growth kinetics measured in diametric compression or in CT specimens

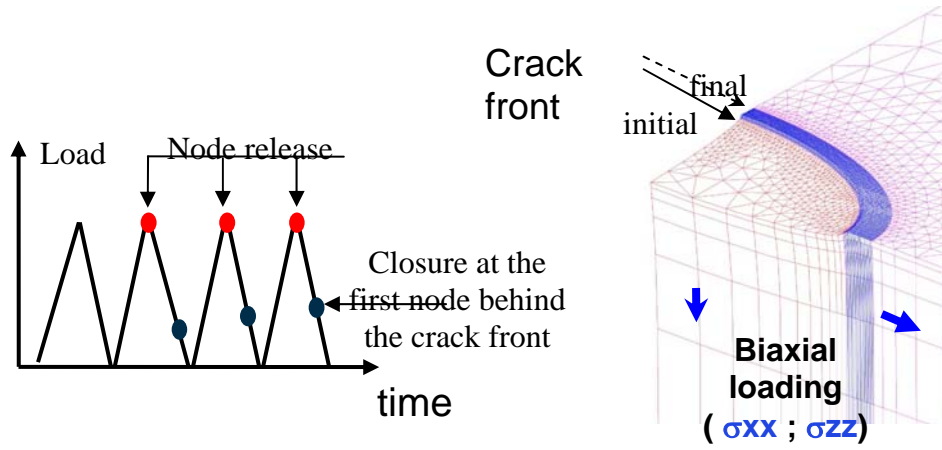


FIGURE 4. Finite elements mesh and procedure used to evaluate  $K_{closure}$

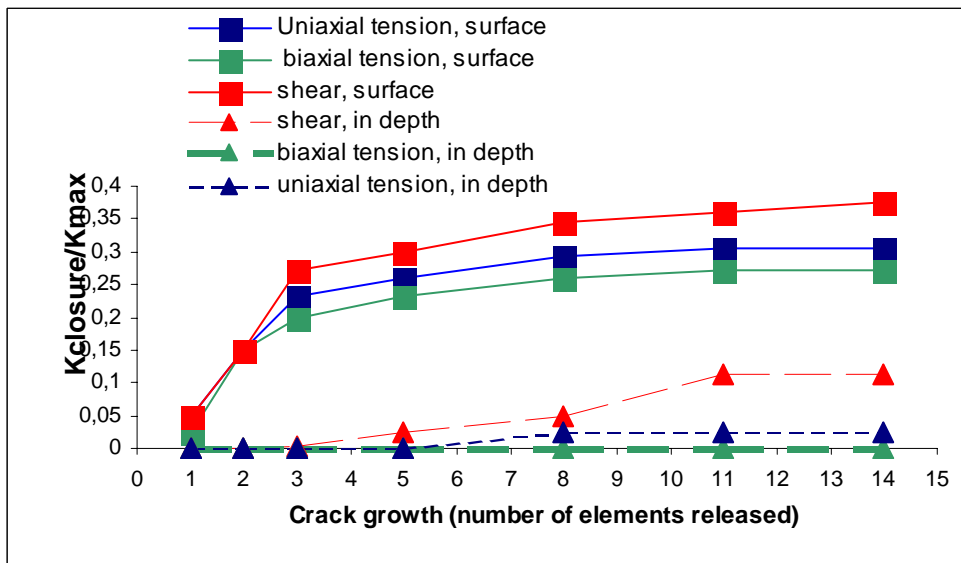


FIGURE 5. Evolution of  $K_{closure}/K_{max}$  with crack growth under biaxial loading

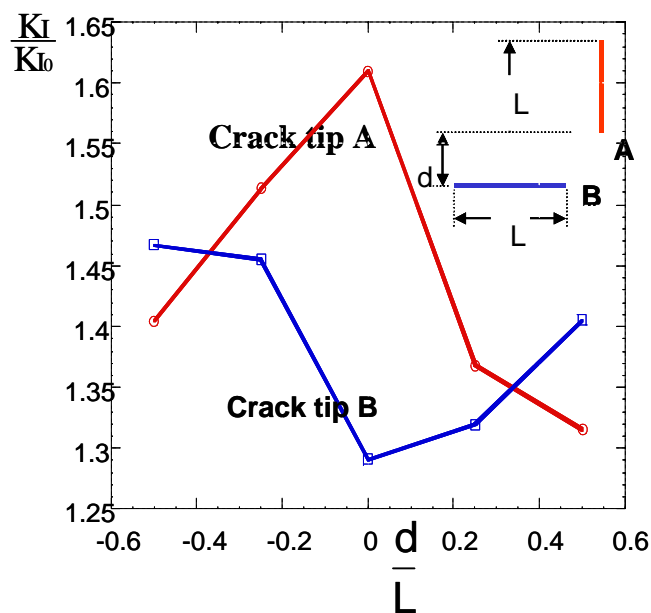


FIGURE 6. Interaction between two orthogonal cracks under equibiaxial tension.

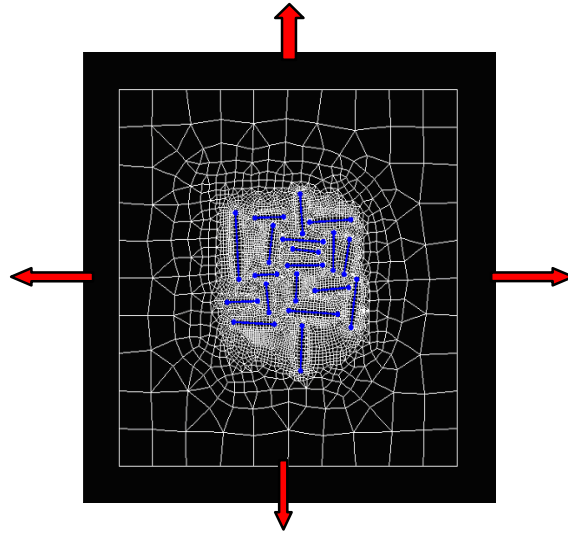


FIGURE 7. Finite element model with 19 cracks loaded in equibiaxial tension.

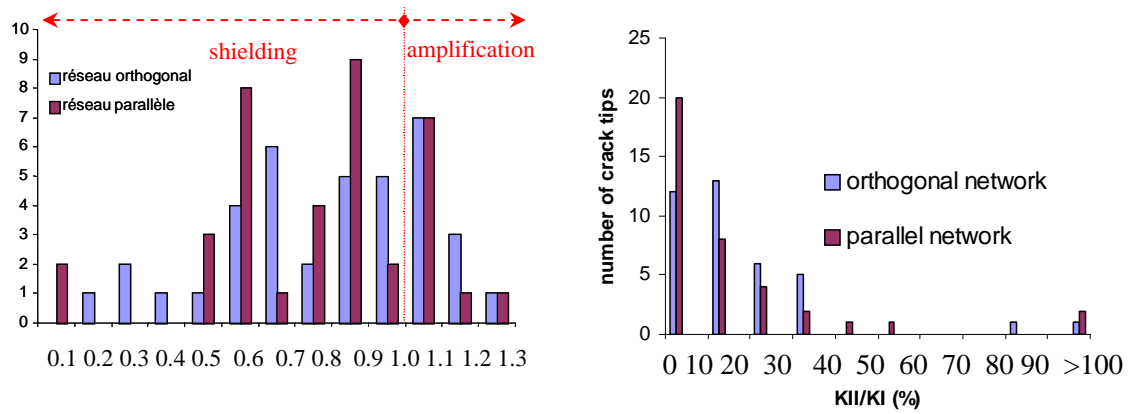


FIGURE 8. Influence of the crack network on a)  $K_I$  b) mode-mixity for the 38 crack tips.

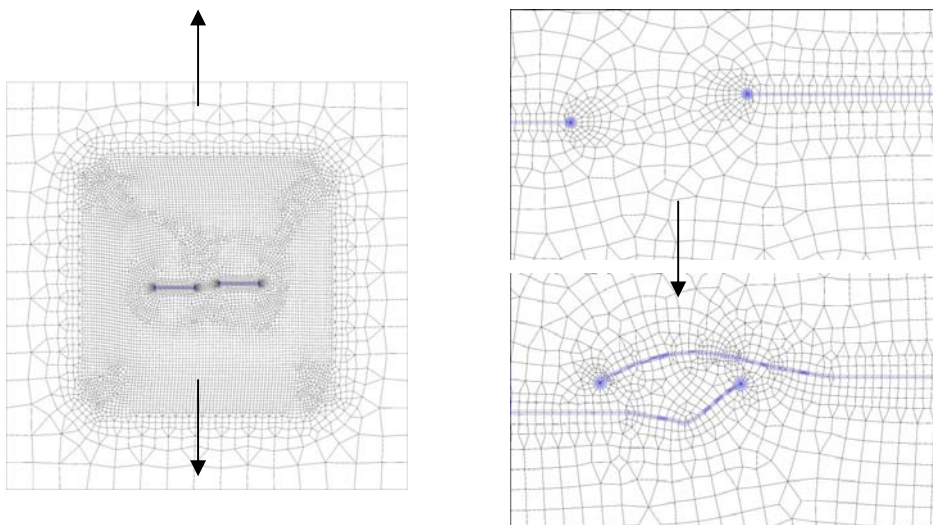


FIGURE 9. Computed evolution of two parallel offset cracks under remote tension